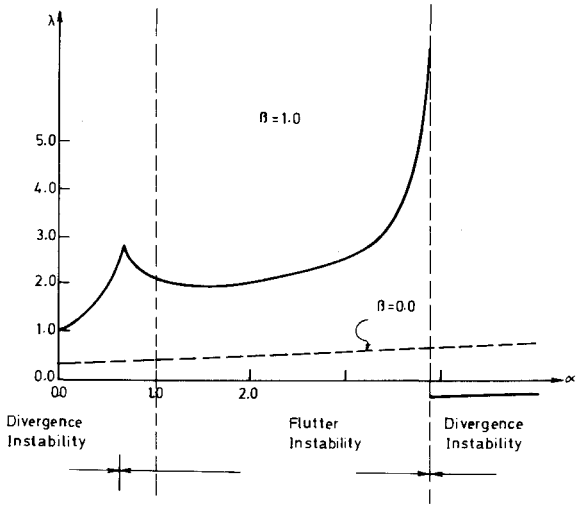

Fig. 3 Variation of critical load with parameter α.

Finally, to investigate the influence of motion-dependency parameters α and β on the magnitude of critical load, we now consider two particular cases of interest. 1) $\beta = 1$, α free to vary. The variation of critical load with parameter α, for this case is plotted in Fig. 3 (solid curves) in which the respective domain of stability criteria is also shown. As an interesting point it is observed that for the subsequent end force ($\beta = 1$), the intermediate force acting through the subtangency α can be considered as a stabilizing agent for certain values of α, shown in this figure. For the sake of comparison, the results of the particular case of constant directional vertical loading ($\beta = 0.0$), which correspond to a conservative force field, are also plotted in this figure. In the latter case the static stability analysis is applicable throughout the whole region. 2) $\alpha = 1$, β free to vary. In this case the variation of the critical force with parameter β in accordance with the static and kinetic criteria is

$$\lambda_s = \frac{3-3\beta \pm (9\beta^2)^{1/2} - 14\beta + 5}{2(1-\beta)}, \quad \beta < 0.556, \quad \beta > 1.0 \qquad (8)$$

and

$$\lambda_k = \frac{8-\beta \pm \{(8-\alpha)^2 - 41[1+(1-\alpha)^2]\}^{1/2}}{2[1+(1-\alpha)^2]} \qquad (9)$$

As noted, Eqs. (8) and (9) are exactly the same as the ones obtained in Ref. 4 for the case of subtangential end loading of the column. In other words, as intuitively expected, a follower state of intermediate loading would have no effect on the stability characteristics of the system.

References

[1] Ziegler, H., "On the Concept of Elastic Stability," *Advances in Applied Mechanics*, Vol. 4, Academic Press, New York, N.Y., 1956, pp. 35–403.

[2] Boltin, V. V., *Non-Conservative Problems of Theory of Elastic Stability*, Pergamon Press, New York, N.Y., 1963.

[3] Kordas, Z. and Zyczkowski, M., "On the Loss of Stability of a Rod Under a Super-Tangential Force," *Archiwum Mechaniki Stosowanej*, Vol. 15, 1963, pp. 7–31.

[4] Herrmann, B. and Bungay, R. W., "On the Stability of Elastic Systems Subjected to Non-Conservative Forces," *Journal of Applied Mechanics*, Vol. 31, Sept. 1964, pp. 435–440.

[5] Herrmann, G. and Jong, I. C., "On the Destabilizing Effect of Damping in Non-Conservative Elastic Systems," *Journal of Applied Mechanics*, Vol. 32, 1965, pp. 592–597.

[6] Herrmann, G., ed., *Dynamic Stability of Structures*, Pergamon Press, New York, N.Y., 1967.

[7] Herrmann, G., "Stability of Equilibrium of Elastic Systems Subjected to Non-Conservative Forces," *Applied Mechanics Review*, Vol. 20, Feb. 1967, pp. 103–108.

[8] Ziegler, H., *Principles of Structural Stability*, Blaisdell Publishing Co., London, 1968, pp. 107–135.

[9] Leipholz, H., "Instability of Continuous Systems," Symposium of International Union of Theoretical and Applied Mechanics, 1969, Springer-Verlag, Berlin, Germany, 1971.

[10] Leipholz, H., *Stability Theory*, Academic Press, New York, N.Y., 1970.

[11] Huseyin, K., "The Elastic Stability of Structural Systems with Independent Loading Parameters," *International Journal of Solids and Structures*, Vol. 6, 1970, pp. 677–691.

[12] Huseyin, H. and Plaut, R. H., "The Elastic Stability of Two Parameter Non-Conservative Systems," *Journal of Applied Mechanics*, March 1973, pp. 175–180.

[13] Farshad, M., "Some Considerations on Timoshenko Bar Problem Subjected to Non-Conservative Loading," *Journal of of Applied Mechanics*, Vol. 41, June 1974, pp. 535–536.

[14] Farshad, M., "On Stability of Coupled Non-Conservative Structural Systems Subjected to Loads with Multiple Motion Dependency," 1974, Dept. of Civil Engineering Report, April 1974, Pahlavi University, Shiraz, Iran.

Boundary-Layer Transition Comparisons in Shock-Induced Flows

JERRY LEE HALL*
Iowa State University, Ames, Iowa

Introduction

THREE methods of ascertaining boundary-layer transition in shock-induced flows are compared in this study: 1) a surface temperature technique using thin-film resistance thermometers; 2) a heat-flux technique using thin-film resistance thermometer recordings and an appropriate relation to convert from surface-temperature histories to heat-flux histories; and 3) schlieren photography of boundary-layer transition. Two shock tubes were used to generate the shock-wave induced boundary layers in order to perform the comparisons. Comparisons are made on the basis of bias introduced into the determination of transition Reynolds number.

The boundary layers in this study are those which develop in two-dimensional unsteady flow over a flat surface (shock tube wall). The governing relations for this flow are given by Mirels[1] and are, with the exception of the boundary condition of finite wall velocity, the typical[2,3] laminar boundary-layer equations. Comparisons in this study are made on the basis of transition Reynolds number as given in Ref. 1. The transition distances or times used to determine transition Reynolds numbers in this study were taken as those conventionally obtained from each of the three techniques for ascertaining transition.

Shock-Tube Facilities

The equipment used in this study consisted of two cold-gas-driven shock-tube facilities, thin-film resistance thermometers with their associated instrumentation and a schlieren photographic system.

Data for comparison of the surface-temperature technique with the heat-flux technique were obtained from a shock tube

Presented as Paper 74-706 at the AIAA/ASME Thermophysics and Heat Transfer Conference, Boston, Massachusetts, July 15–17, 1974; submitted August 9, 1974; revision received October 17, 1974. This work was supported by the Engineering Research Institute and the Mechanical Engineering Department at Iowa State University, Ames, Iowa.

Index category: Boundary-Layer Stability and Transition.

* Associate Professor. Member AIAA.

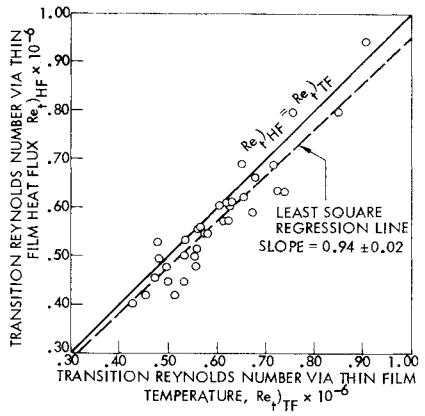

Fig. 1 Comparison of thin-film and heat-flux transition Reynolds numbers.

(shock tube No. 1) consisting of a cylindrical stainless steel driver section of 78 mm internal diam and 1177 mm long. The driven section, except for the test section, was constructed of reinforced waveguide tubing with a 37×74 mm rectangular internal cross section and a length of 3600 mm. Transition data was obtained from a thin film located 182 mm from the downstream end of this shock tube.

Data for comparison of the surface temperature technique with the schlieren technique was obtained from a shock tube (shock tube No. 2) consisting of a cylindrical driver section of 178 mm internal diam and 1829 mm long. The driven section was constructed of aluminum plates with a 76×152 mm rectangular internal cross section and a length of 9144 mm. Transition data with this shock tube were obtained from both a schlieren system and a thin-film located 203 mm from its downstream end.

Range of the Experiments

For each shock tube, the freestream flow properties were varied by selecting initial test-gas pressures (p_1) from 5–50 torr and by controlling shock-wave strength through selection of different thickness of Mylar diaphragms. In this way a continuum gas-dynamic flow was generated with freestream pressures ranging from 100–1100 torr and shock wave Mach numbers from 3.0–5.5. These ranges of pressure and Mach number kept the freestream temperatures between 900 and 2100°K. The shock-tube driver gas was helium and the test gas was nitrogen for these experiments. Helium was required as a driver gas in order to attain the desired pressures, temperatures, and Mach numbers.

Transition Measurements

Contact Surface Limitation

The transition times or distances used in this study to determine transition Reynolds numbers were all obtained under carefully monitored conditions where there was no possibility of the interface (contact surface) preceding transition of the boundary layer. Also, for verification, the schlieren photographs of this study would have shown evidence of this contact surface had it been present. The field of view of this schlieren system was approximately 15 cm wide, and transition occurred within a few centimeters after the incident shock wave. Thus, the transition times in these experiments are much less than shock-tube testing times (interface arrival), which precludes this effect from causing transition. The transition regime periods for these experiments were all less than 160 μsec.

Thin-Film Techniques

Platinum thin-film resistance thermometers were used to obtain surface-temperature histories and transition data according to established techniques.[4,5] Description of the construction and use of such thin-film resistance thermometers is contained in existing literature.[6,7] In these experiments, thin films were flush mounted in the wall of the shock-tube test section allowing measurements of shock-wave velocity as well as surface-temperature history. The transition for this technique was taken when the thin films indicated a departure from the characteristic constant wall temperature such as is indicative of a laminar shock induced boundary layer.[4]

Heat-Transfer Technique

Surface heat-transfer rates are calculated from surface-temperature histories via oscilloscope recordings of output voltage signals from thin-film resistance thermometers.[8] This technique is different from others using thin-film resistance thermometers, because heat-transfer rate history is used to determine transition rather than surface-temperature history. The advantage of using heat-transfer rate is that it depends on temperature gradient at the surface and is therefore more sensitive than temperature level. This is extremely important when the thin-film output does not indicate a sudden temperature change at transition but instead a monotonically increasing temperature change. With this condition, using temperature level to determine transition may not be sensitive enough to give unbiased transition points compared to the heat-transfer technique. Furthermore, the heat-transfer technique shows the entire transition process.

Schlieren Technique

Transition distances obtained from schlieren photographs are converted to appropriate transition times for comparison with corresponding transition times obtained from thin-film recordings during the same experimental run. Transition distances by this technique are taken when the first departure from a laminar layer is observed.

Results

Heat Flux Comparison

Figure 1 is a comparison of transition Reynolds numbers obtained by the heat-flux technique with those obtained simultaneously from thin-film recordings. Study of this figure reveals the heat-flux technique to generally yield smaller transition times than the thin-film recordings for the same experimental run. This general bias plus random error (data scatter) is no larger than 20% for this data. Note in this figure that the scatter is indicative of random error in the measurements and should occur about a line of unity slope (equal scales on both axes) if there is no bias in the methods being compared. With bias the scatter will occur about a line whose slope is indicative of the amount of bias. A least-square curve fit of the data in Fig. 1 yields a line of slope 0.94 ± 0.02 at the 95% confidence level. Thus, there is a 6% bias in obtaining transition times by one technique as compared to another.

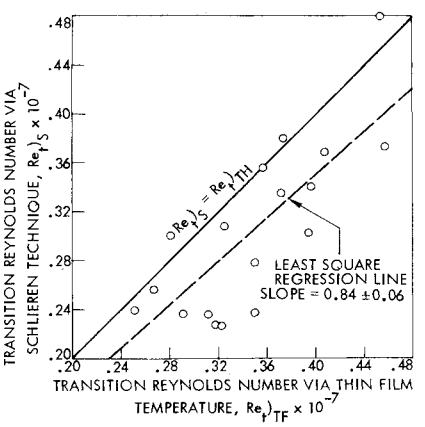

Fig. 2 Comparison of thin-film and schlieren transition Reynolds numbers.

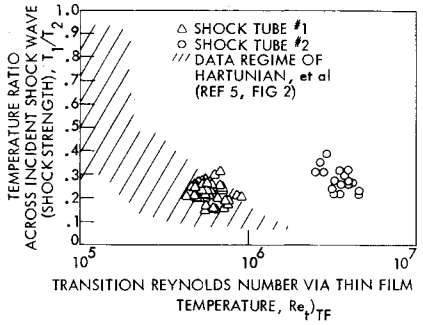

Fig. 3 Comparison of transition data with previous literature.

It is important to emphasize that this bias occurs regardless of the magnitude of the random error. When the random error is relatively large the bias tends to be obscured. But when the random error is relatively small the bias becomes evident and emphasizes the need for care in selection of instrumentation and data reduction procedures.

Schlieren Comparison

Figure 2 is a comparison of transition times obtained from schlieren photographs with those obtained simultaneously from thin-film recordings. This figure reveals the schlieren technique to generally yield lower transition times than the thin-film recordings for the same experimental run. In this case the bias plus random error (data scatter) is a maximum of about 50%. The least square line fitting this data has a slope of 0.84 ± 0.06 with 95% confidence. Thus, the bias is about 16% in this case. The additional scatter in the data is caused by difficulty in reading or determining transition from the schlieren photographs.

Comparison with Previous Literature

Figure 3 is a comparison of the thin-film transition data from these experiments with a summary of earlier transition data presented by Harturian, Russo, and Marrone.[5] The cross-hatched portion of Fig. 3 shows both the range and scatter of the data presented in Ref. 5. Different symbols are used to represent the data from each shock-tube facility used in these experiments. Figure 3 shows good agreement of transition data through transition Reynolds numbers of 10^6.

An apparent transition reversal is noted in Fig. 3 where, from shock tube No. 2, at a lower freestream temperature (smaller heat flux to the wall) the transition Reynolds numbers are extended to above values available for comparison with existing literature as well as those obtained in shock tube No. 1. This effect is well known to exist in conventional steady flow boundary layers but has only been reported in the literature[8] for shock induced boundary layers where heat flux has been incident on the boundary layer from combustion reactions occurring in the mainstream. Some difference in transition Reynolds number from each shock tube should be expected between these facilities because of uncontrolled factors in these experiments such as freestream turbulence, surface roughness, three-dimensional effects, and shock tube size.[3,9] Even though these differences are not quantified in these experiments the data from shock tube No. 1 compares well with the data of Ref. 5 which was obtained from a variety of facilities where, in some cases, the experimental conditions were carefully controlled. Thus, since the differences noted in Fig. 3 are larger than the possible uncertainties in the data, this reversal effect is believed to be real and is reported herein for your consideration.

References

[1] Mirels, H., "Laminar Boundary Layer Behind a Strong Shock Moving into Air," TN D-291, Feb. 1961, NASA.

[2] Wilson, R., "Viscosity and Heat Transfer Effects," *Handbook of Supersonic Aerodynamics*, Vol. 5, Sec. 13–14, U.S. Bureau of Naval Weapons NAVORD Rept. 1488, 1966.

[3] Davies, W. R. and Bernstein, L., "Heat Transfer and Transition to Turbulence in the Shock Induced Boundary Layer on a Semi-Infinite Flat Plate," *Journal of Fluid Mechanics*, Vol. 36, Pt. 1, March 1969, pp. 87–112.

[4] Bromberg, R., "Use of the Shock Tube Wall Boundary Layer in Heat Transfer Studies," *Jet Propulsion*, Vol. 26, Sept. 1956, pp. 737–740.

[5] Hartunian, R., Russo, A., and Marrone, P., "Boundary-Layer Transition and Heat Transfer in Shock Tubes," *Journal of the Aerospace Sciences*, Vol. 27, Aug. 1960, pp. 587–594.

[6] Henshall, B. and Schultz, D., "Some Notes on the Use of Resistance Thermometers for Measurement of Heat-Transfer Rates in Shock Tubes," Great Britain Aeronautical Research Council Current Paper 408, London, England, 1959.

[7] Taylor, B., "Development of a Thin Film Heat-Transfer Gauge For Shock Tube Flows," Technical Note 27, Institute of Aerophysics, University of Toronto, Toronto, Canada, 1959.

[8] Hall, J. L., Serovy, G. K., and Belles, F., "Effects of Heat Energy Release from Shock Induced Exothermic Reactions on Boundary Layer Transitions in Shock-Tube Flows," *Heat Transfer 1970*, Vol. III, Paper FC 9.2, Fourth International Heat Transfer Conference, Paris-Versailles, France, 1970.

[9] Braslow, A. L., "A Review of Factors Affecting Boundary-Layer Transition," TN D-3384, Aug. 1966, NASA.

Minimum Length Axisymmetric Laval Nozzles

LUCIAN Z. DUMITRESCU*
Institute of Fluid Mechanics and Aerospace Technology, Bucharest, Romania

I. Introduction

THIS paper deals with the determination of a class of minimum-length axisymmetric Laval nozzles, which are compared to the simple conical type, emphasizing the extra length needed to ensure uniform flow conditions. Submission of the paper has been prompted by the publication of Ref. 1; in fact, most of the following results have been obtained (and applied) over ten years ago, including the derivation of the hodograph equation for axisymmetric source flow, Eq. (4), but were left dormant in a journal of limited circulation.[2]

II. Basic Equations

Referring to Fig. 1, consider a spherical source flow, which is supersonic at distances r greater than the critical radius r_c. Writing that the mass flow m is constant at any distance:

$$4\pi r^2 \rho V = m = \text{const} \tag{1}$$

one obtains readily (see, e.g., Ref. 3, p. 372):

$$R^2 = (r/r_c)^2 = \frac{1}{M}\left(\frac{2}{\gamma+1} + M^2\right)^{(\gamma+1)/2(\gamma-1)} \tag{2}$$

Now, along a characteristic line BB' of this source flow, the velocity vector makes an angle $\mu = \text{arc sin}\,(1/M)$ with the local tangent. Therefore, one has:

$$r\,d\theta/dr = -tg\mu = -1/(M^2-1)^{1/2} \tag{3}$$

But the ratio dr/r may be obtained by differentiating Eq. (2). After integration of Eq. (3) the following fundamental formula results:

Received June 5, 1975.
Index categories: Nozzle and Channel Flow; Supersonic and Hypersonic Flow.

* Senior Scientist; Head, Shock-Tube Laboratory.